AMERICAN SOCIETY FOR MICROBIOLOGY | mBio®

RESEARCH ARTICLE

Flavivirus Infection of *Ixodes scapularis* (Black-Legged Tick) *Ex Vivo* Organotypic Cultures and Applications for Disease Control

Jeffrey M. Grabowski,[a] Konstantin A. Tsetsarkin,[b] Dan Long,[c] Dana P. Scott,[c] Rebecca Rosenke,[c] Tom G. Schwan,[d] Luwanika Mlera,[a] Danielle K. Offerdahl,[a] Alexander G. Pletnev,[b] Marshall E. Bloom[a]

Biology of Vector-Borne Viruses Section, Laboratory of Virology, Rocky Mountain Laboratories, NIAID, NIH, Hamilton, Montana, USA[a]; Neurotropic Flaviviruses Section, Laboratory of Infectious Diseases, NIAID, NIH, Bethesda, Maryland, USA[b]; Rocky Mountain Veterinary Branch, Rocky Mountain Laboratories, NIAID, NIH, Hamilton, Montana, USA[c]; Laboratory of Zoonotic Pathogens, Rocky Mountain Laboratories, NIAID, NIH, Hamilton, Montana, USA[d]

ABSTRACT *Ixodes scapularis* ticks transmit many infectious agents that cause disease, including tick-borne flaviviruses (TBFVs). TBFV infections cause thousands of human encephalitis cases worldwide annually. In the United States, human TBFV infections with Powassan virus (POWV) are increasing and have a fatality rate of 10 to 30%. Additionally, Langat virus (LGTV) is a TBFV of low neurovirulence and is used as a model TBFV. TBFV replication and dissemination within *I. scapularis* organs are poorly characterized, and a deeper understanding of virus biology in this vector may inform effective countermeasures to reduce TBFV transmission. Here, we describe short-term, *I. scapularis* organ culture models of TBFV infection. *Ex vivo* organs were metabolically active for 9 to 10 days and were permissive to LGTV and POWV replication. Imaging and videography demonstrated replication and spread of green fluorescent protein-expressing LGTV in the organs. Immunohistochemical staining confirmed LGTV envelope and POWV protein synthesis within the infected organs. LGTV- and POWV-infected organs produced infectious LGTV and POWV; thus, the *ex vivo* cultures were suitable for study of virus replication in individual organs. LGTV- and POWV-infected midgut and salivary glands were subjected to double-stranded RNA (dsRNA) transfection with dsRNA to the LGTV 3′ untranslated region (UTR), which reduced infectious LGTV and POWV replication, providing a proof-of-concept use of RNA interference in *I. scapularis* organ cultures to study the effects on TBFV replication. The results contribute important information on TBFV localization within *ex vivo I. scapularis* organs and provide a significant translational tool for evaluating recombinant, live vaccine candidates and potential tick transcripts and proteins for possible therapeutic use and vaccine development to reduce TBFV transmission.

IMPORTANCE Tick-borne flavivirus (TBFV) infections cause neurological and/or hemorrhagic disease in humans worldwide. There are currently no licensed therapeutics or vaccines against Powassan virus (POWV), the only TBFV known to circulate in North America. Evaluating tick vector targets for antitick vaccines directed at reducing TBFV infection within the arthropod vector is a critical step in identifying efficient approaches to controlling TBFV transmission. This study characterized infection of female *Ixodes scapularis* tick organ cultures of midgut, salivary glands, and synganglion with the low-neurovirulence Langat virus (LGTV) and the more pathogenic POWV. Cell types of specific organs were susceptible to TBFV infection, and a difference in LGTV and POWV replication was noted in TBFV-infected organs. This tick organ culture model of TBFV infection will be useful for various applications,

Received 19 July 2017 **Accepted** 25 July 2017 **Published** 22 August 2017

Citation Grabowski JM, Tsetsarkin KA, Long D, Scott DP, Rosenke R, Schwan TG, Mlera L, Offerdahl DK, Pletnev AG, Bloom ME. 2017. Flavivirus infection of *Ixodes scapularis* (black-legged tick) *ex vivo* organotypic cultures and applications for disease control. mBio 8:e01255-17. https://doi.org/10.1128/mBio.01255-17.

Editor Vincent R. Racaniello, Columbia University College of Physicians and Surgeons

Address correspondence to Marshall E. Bloom, mbloom@niaid.nih.gov.

This article is a direct contribution from a Fellow of the American Academy of Microbiology. Solicited external reviewers: Ulrike Munderloh, University of Minnesota; Alan Barrett, University of Texas Medical Branch.

such as screening of tick endogenous dsRNA corresponding to potential control targets within midgut and salivary glands to confirm restriction of TBFV infection.

KEYWORDS Langat virus, Powassan virus, RNA interference, dsRNA, metabolism, midgut, organ, prevention, salivary gland, synganglion, vaccines, virus

Ixodid ticks (subphylum *Chelicerata*, subclass *Acari*, family *Ixodidae*) are vectors for numerous pathogens of human diseases. Some well-known examples are *Borrelia burgdorferi*, a cause of Lyme disease, *Rickettsia rickettsii*, the cause of Rocky Mountain spotted fever, *Francisella tularensis*, the cause of tularemia, and a number of other viruses, including the tick-borne flaviviruses (TBFVs) (1–8).

The TBFVs comprise a group of about seven viruses that can cause serious, sometimes fatal, human infections. The tick-borne encephalitis viruses (TBEVs) and Powassan virus (POWV lineage I [LB strain] and lineage II [Deer tick virus strain; DTV]) cause severe meningoencephalitis, whereas Langat virus (LGTV) has low neurovirulence in humans (7, 9–12). LGTV was first isolated from *Ixodes granulatus* ticks in Malaysia (13), and no confirmed natural LGTV disease cases have been identified. Infections with other TBFVs, like Kyasanur Forest disease virus (KFDV), Omsk hemorrhagic fever virus (OHFV), and Alkhurma hemorrhagic fever virus (AHFV), manifest as a serious hemorrhagic fever syndrome. The case fatality rate from TBFV infections can range as high as 20% (9, 14), and there can also be considerable morbidity and long-term sequelae. POWV lineages I and II are the only TBFVs autochthonous in North America (15–17), and an increase in the number of human POWV disease cases in the United States has been observed since 1999 (15, 18, 19). The diseases caused by these viruses are well characterized, and the experimental biology and pathogenesis of TBFV infections in mammalian hosts have been reasonably well studied.

The biology of TBFVs in arthropod hosts is not as well studied. The tick hosts associated with TBFVs are almost exclusively hard ticks, although AHFV was isolated from the soft-bodied tick *Ornithodoros savignyi*. POWV has been isolated from wild populations of ticks in North America (20–23), specifically, *Ixodes marxi*, *Ixodes cookei*, *Ixodes spinipalpis*, *Ixodes scapularis*, and *Dermacentor andersoni* (7, 8, 15, 24–26). Furthermore, *I. scapularis* and *D. andersoni* are competent vectors for POWV in laboratory studies (27–29). Interestingly, transovarial transmission of POWV was observed with *I. scapularis*, but not with *D. andersoni* ticks (15, 28). Although LGTV has not been naturally isolated from *I. scapularis*, this tick species is a competent experimental vector for the virus (30).

TBFVs can be maintained transstadially and transovarially through the tick's life cycle, and TBFVs may spend 95% of their evolutionary life span in the tick host (30–32). In spite of this, there are limited studies of the biology of TBFV infections in ticks. Although tick cell culture is extremely useful in virus infection studies (33, 34), limitations exist with *in vitro* cell cultures (passaging of tick cells may cause the cells to deviate further from their natural state, and cell populations of a single cell type do not necessarily represent multicellular organ tissues within the tick), and combining *in vitro*, *ex vivo*, and/or *in vivo* approaches is advisable. Specifically, the exact types of cells that can be infected with TBFVs in the tick midgut, salivary glands, and synganglion remain undetermined. Since TBFV infection changes tick behavior (35, 36) and transcript expression of salivary glands (37), this information would be extremely useful. One approach is the use of *ex vivo* tick organ cultures, where TBFV infection can be tightly controlled and readily investigated; however, few investigators have used this approach. Two studies demonstrated TBFV replication in *Hyalomma* sp. tick tissue explants (38, 39), and another study investigated replication of Semliki Forest virus (a member of the *Togaviridae* family) in *Rhipicephalus* sp. tick tissue explants (40). In addition, little is known about the short-term culture and viability of dissected, individual tick organs, especially those of *I. scapularis*, or if these organ cultures can be productively infected. Thus, tick organ cultures might be valuable avenues for studying virus infections in ticks.

Another research area in which tick organ cultures might be valuable tools is the knockdown of tick gene expression by RNA interference (RNAi). For example, soaking *Amblyomma americanum* midgut sections and salivary glands with double-stranded RNA (dsRNA) that targets endogenous gene transcripts reduces transcript expression (41–45). Because of the importance of *I. scapularis* in a variety of infections, the effect of dsRNA treatment on TBFV replication and organ viability is important to evaluate. Although specific *Ixodes* spp. transcripts have been implicated in TBFV infection in tick cell cultures (46–48), *ex vivo* organ cultures can provide a means to more precisely probe tissue-specific vector interactions.

In this study, we dissected midgut, salivary glands, and synganglion from female *I. scapularis* ticks and confirmed that the organs were viable in *ex vivo* culture for over a week. Furthermore, we infected the organ cultures with LGTV and POWV, demonstrated virus dissemination, and identified production of infectious virus. We also transfected dsRNA targeting the LGTV 3′ untranslated region (UTR) into organ cultures of TBFV-infected midgut and salivary gland tissues and observed a reduction in TBFV replication. Thus, we developed a tick organ culture model that can be applied as a functional genomics tool for studying TBFV biology and screening for vaccine or drug candidates. The organ culture model may also prove useful for high-containment studies where working with live ticks and select agents may be challenging.

RESULTS

Viability of dissected *I. scapularis* organs. The overarching goal of our study was to develop an organotypic culture model of isolated organs from the adult *I. scapularis* female tick to study the biology of TBFVs. The initial step was to determine the viability of these organs in culture, using a resazurin salt-based viability assay (48, 49). Dissected midgut and salivary glands were viable for up to 240 h (10 days), whereas synganglion specimens were viable for up to 216 h (9 days) (Fig. 1A to C). Thus, these three organs were metabolically active for a time sufficient to study *ex vivo* virus infection.

Infection of tick organ cultures with a GFP-expressing LGTV. The next step was to analyze whether the dissected tick organ cultures would support infection and spread of TBFV. We infected midgut, salivary gland, and synganglion cultures with LGTV expressing green fluorescent protein (LGTV^{GFP}) and observed the cultures by live fluorescence microscopy, using the GFP signal as an indicator of virus infection and gene expression. The growth of recombinant flaviviruses may differ from parental viruses (50, 51); however, the potential difference in growth between LGTV^{GFP} and its wild-type LGTV TP21 strain in these organs has not been determined.

GFP expression was observed in midgut (Fig. 2; see also Movie S1 and S3 in the supplemental material), salivary gland (Fig. 3), and synganglion (Fig. 4) cultures at selected time points postinfection. Nonspecific autofluorescence was observed in both LGTV^{GFP}-infected and mock-infected organs and was especially high in the synganglion, but background fluorescence was distinguishable from GFP expression from LGTV^{GFP} at different time points in different organs. LGTV^{GFP} replication was first noted in the midgut tissue (MGT) at 72 hours postinfection (hpi) (Fig. 2; Movie S1) and in salivary gland tissue at 108 hpi (Fig. 3), but not until 180 hpi in synganglion tissue (Fig. 4) in one imaging experiment. In addition, midgut cultures exhibited peristaltic contractions (Movie S1, S2, S3 and S4), a finding typical for this specific organ type, and these were consistently seen at multiple time points. Evidence of virus spread, manifested by spreading GFP expression, was observed from earlier to later time points (Fig. 2, 3, and 4; Movie S1 and S3).

In the midgut, LGTV^{GFP} replication, observed via GFP expression, was seen diffusely throughout the diverticula of the midgut (Fig. 2; Movie S1 and S3). This suggested that the epithelial cells (consisting of reserve, secretory, and digestive cells) (52, 53) were likely targeted by the virus, although the specific infected cell type was not identified. GFP expression in the salivary gland appeared as puncta, primarily along lobular ducts and within acini (Fig. 3); however, we were unable to identify the specific type of acinus

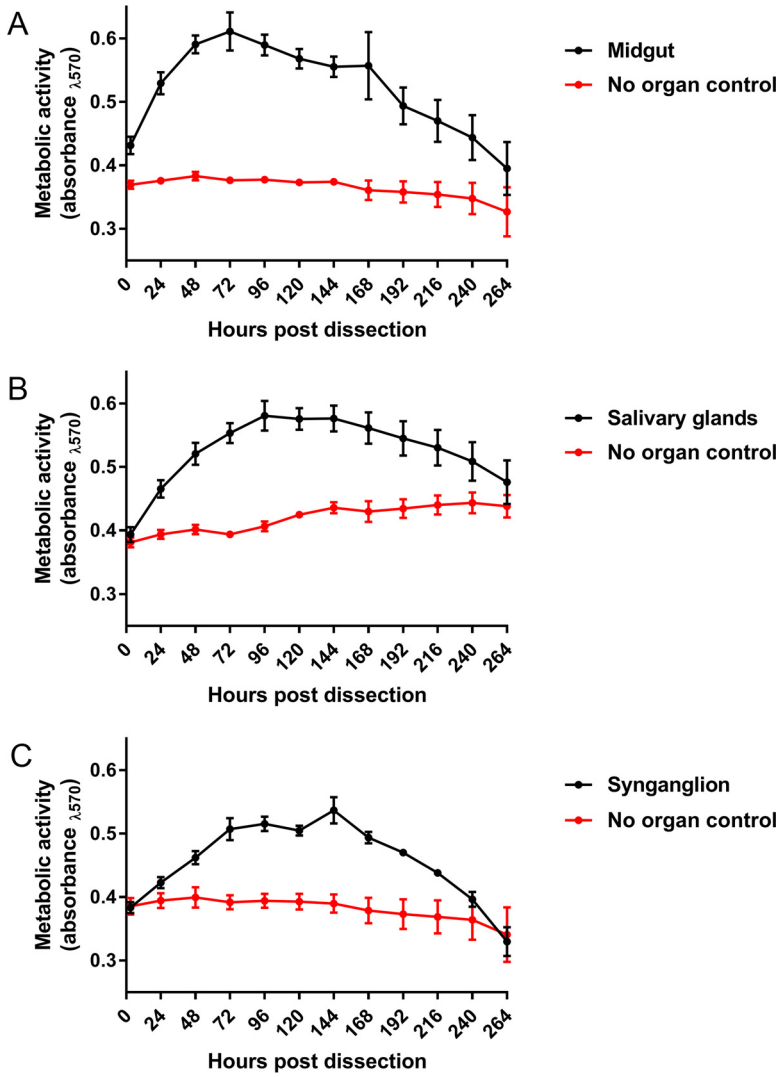

FIG 1 Metabolic activity of dissected organ cultures. Cell viability readings were completed with either one midgut (A), one salivary gland pair (B), or one synganglion (C) with its corresponding control for all time points. Error bars represent standard errors of the means, and data are representative of two machine replicates for each sample during viability reads of three biological replicates.

(54–56) in our experiment. GFP expression in synganglion localized in puncta in residual MGT as well as in the retrocerebral area (RCA) of the synganglion (Fig. 4).

Detection of LGTV and POWV protein synthesis in infected organ cultures. The experiments with LGTV^{GFP} indicated that the virus infected the midgut, salivary glands, and synganglion. Spread of virus infection was noted in the midgut and salivary glands. In order to confirm these results with an independent method and to compare infection of LGTV with that by a pathogenic TBFV, we infected cultures with either LGTV or POWV and prepared samples for immunohistochemical staining every 48 h between 48 hpi and 192 hpi.

The infected organ sections were stained either with an anti-LGTV envelope (E) antibody or with a mouse polyclonal antiserum that recognizes multiple POWV proteins. Staining specific for LGTV or POWV was observed in infected organs (Fig. 5 and 6; Fig. S1 and S2), but not in mock-infected organs (Fig. S3). In addition, spread of LGTV and POWV proteins was observed in infected midgut and salivary gland cells from earlier to later time points, but spread of TBFV proteins within synganglion (other than at the time of first observation of proteins) was not clearly shown (Fig. 5 and 6).

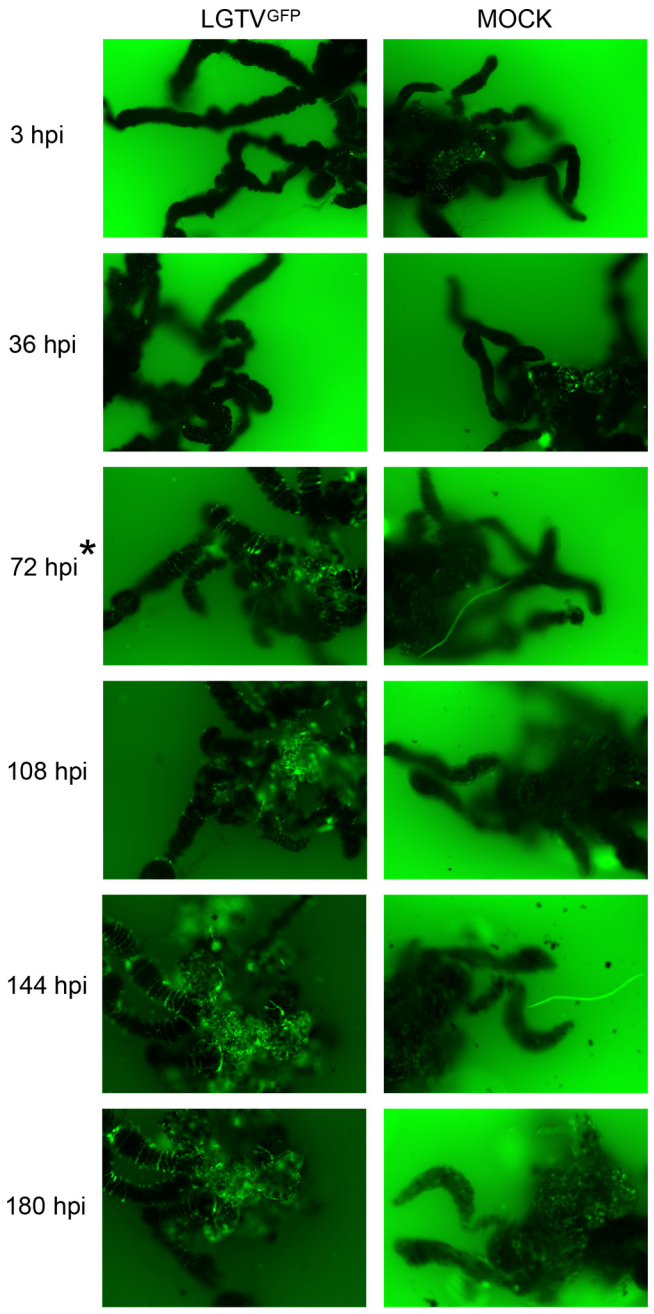

FIG 2 LGTV^{GFP} replication in infected midgut culture. Magnification, ×10 for organs with GFP filter imaging. LGTV expressed GFP, shown in green within the organ. A mock-infected organ was used for comparison, and small amounts of autofluorescence were observed. Serial imaging of the same LGTV^{GFP}-infected and mock-infected midgut organ was performed. The asterisk at 72 hpi denotes the first time point where GFP expression within the LGTV^{GFP}-infected midgut was distinguishable from autofluorescence in the mock-infected midgut.

Localization of LGTV and POWV proteins was similar in all three organ types. LGTV E and POWV protein synthesis in the midgut were initially observed at 48 hpi (Fig. 5) and 96 hpi (Fig. 6), respectively. Epithelial cells of the midgut diverticulum were infected, as indicated by the presence of viral proteins (Fig. S1), but again, specific infected cell types were not identified. LGTV E and POWV protein synthesis in the salivary gland were also initially observed at 48 hpi (Fig. 5) and 96 hpi (Fig. 6), respectively. Primary areas of viral protein synthesis in salivary glands were localized to cells lining the lobular ducts and granular acinus types II and/or III (54–56). LGTV E and

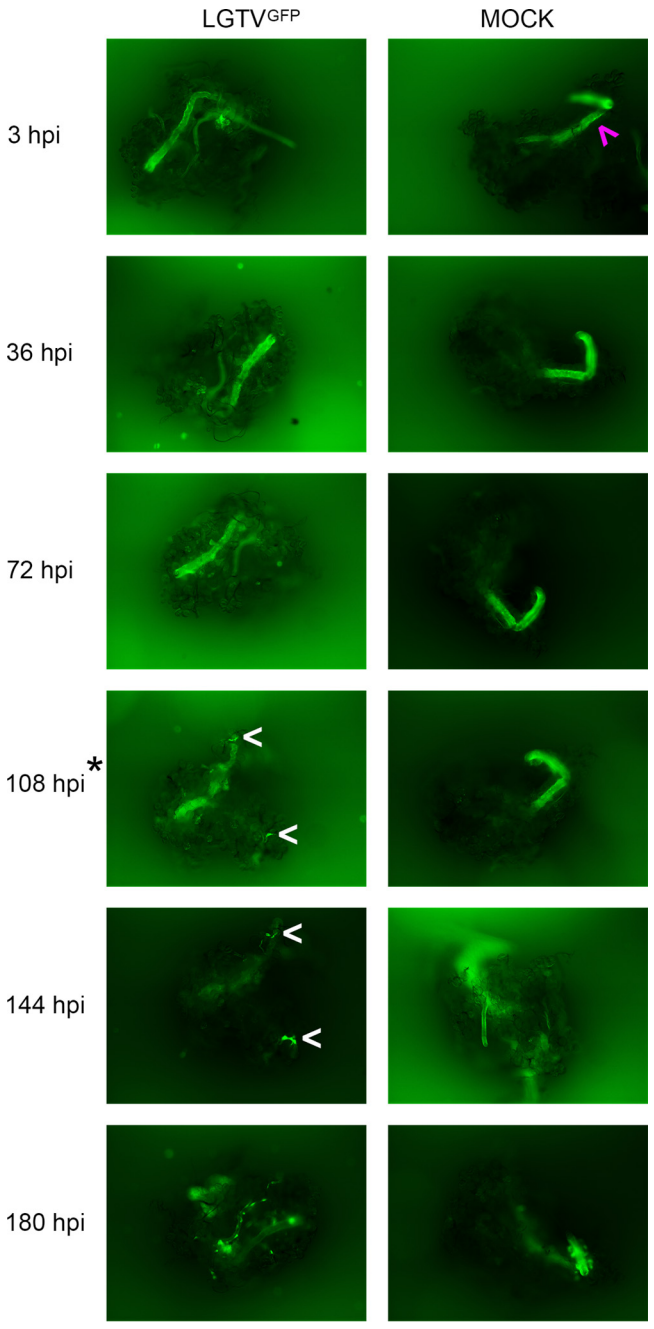

FIG 3 LGTV^{GFP} replication in infected salivary gland culture. Magnification, ×10 (organ with GFP filter imaging). LGTV expressed GFP, shown in green within the organ. Mock-infected organs were used for comparison, and small amounts of autofluorescence were observed within the lobular duct (ld; denoted by magenta arrow). Serial imaging of the same LGTV^{GFP}-infected and mock-infected midgut organ was completed. White arrows denote GFP puncta within LGTV^{GFP}-infected salivary glands. A great amount of GFP puncta were observed at 180 hpi (white arrows were not used). The asterisk at 108 hpi denotes the first time point where GFP expression within LGTV^{GFP}-infected salivary glands was distinguishable from autofluorescence in mock-infected salivary glands.

POWV protein synthesis in the synganglion was initially observed at 144 hpi (Fig. 5) and 96 hpi (Fig. 6), respectively. LGTV E and POWV protein synthesis in the synganglion localized both in the MGT and in the periganglionic sinus/sheath (PGS/H). POWV protein synthesis was also observed in the RCA (Fig. 6) of synganglion.

Infectious LGTV and POWV replication in organ cultures. In the previous sections, we utilized two different methods to demonstrate TBFV infection and gene

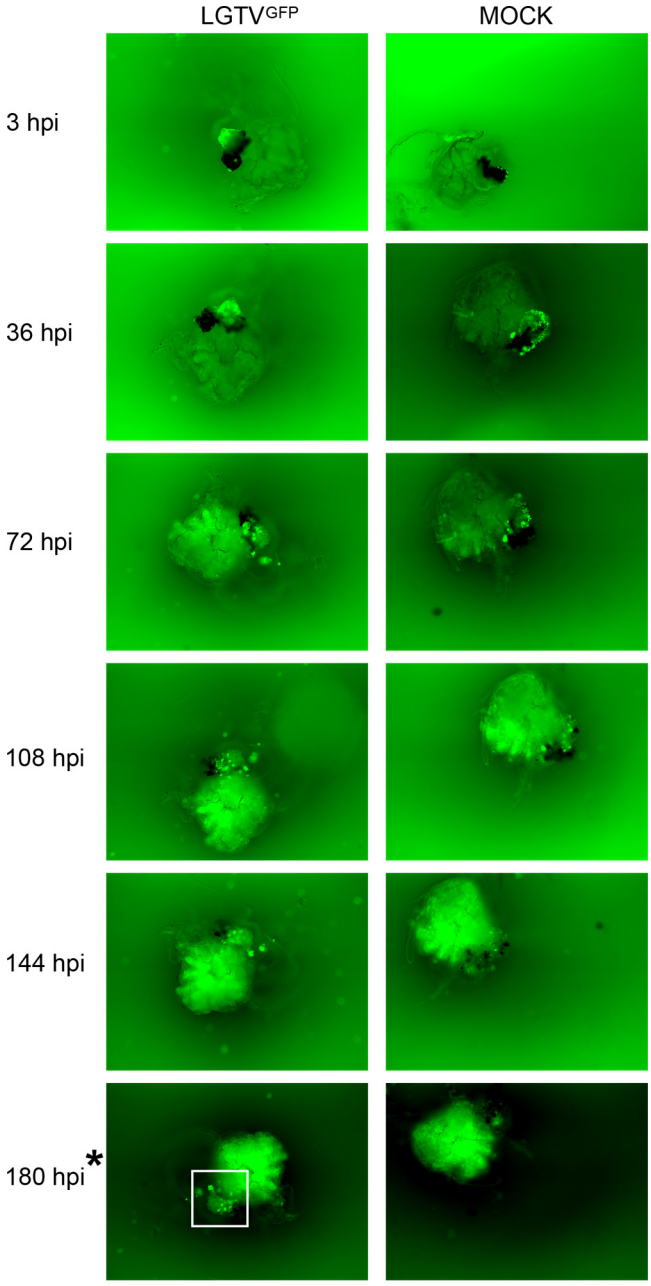

FIG 4 LGTV^{GFP} replication in infected synganglion culture. Magnification, ×10 (organ with GFP filter imaging). LGTV expressing GFP is denoted by green within the organ. A mock-infected organ was used for comparison, and high autofluorescence was observed. Serial imaging of the same LGTV^{GFP}-infected and mock-infected midgut organ was performed. The white box denotes GFP puncta within LGTV^{GFP}-infected synganglion in midgut tissue and in the retrocerebral area. The asterisk at 180 hpi denotes the time point where puncta of GFP expression within LGTV^{GFP}-infected synganglion was distinguishable from autofluorescence in mock-infected synganglion.

expression within dissected tick organ cultures. To determine if infectious virus was being produced, we next employed an immunofocus assay (57–59) to evaluate if virus was generated in these cultures.

Organ cultures were infected with 5×10^5 focus-forming units (FFU) of either LGTV or POWV, a sufficient concentration to establish TBFV infection in *Ixodes* spp. ticks (30, 60, 61). Infectious LGTV and POWV were produced from all three infected tick organ cultures (Fig. 7 and 8). All infected organ types produced greater infectious virus replication than the initial inoculum control (with no organs) at multiple time points

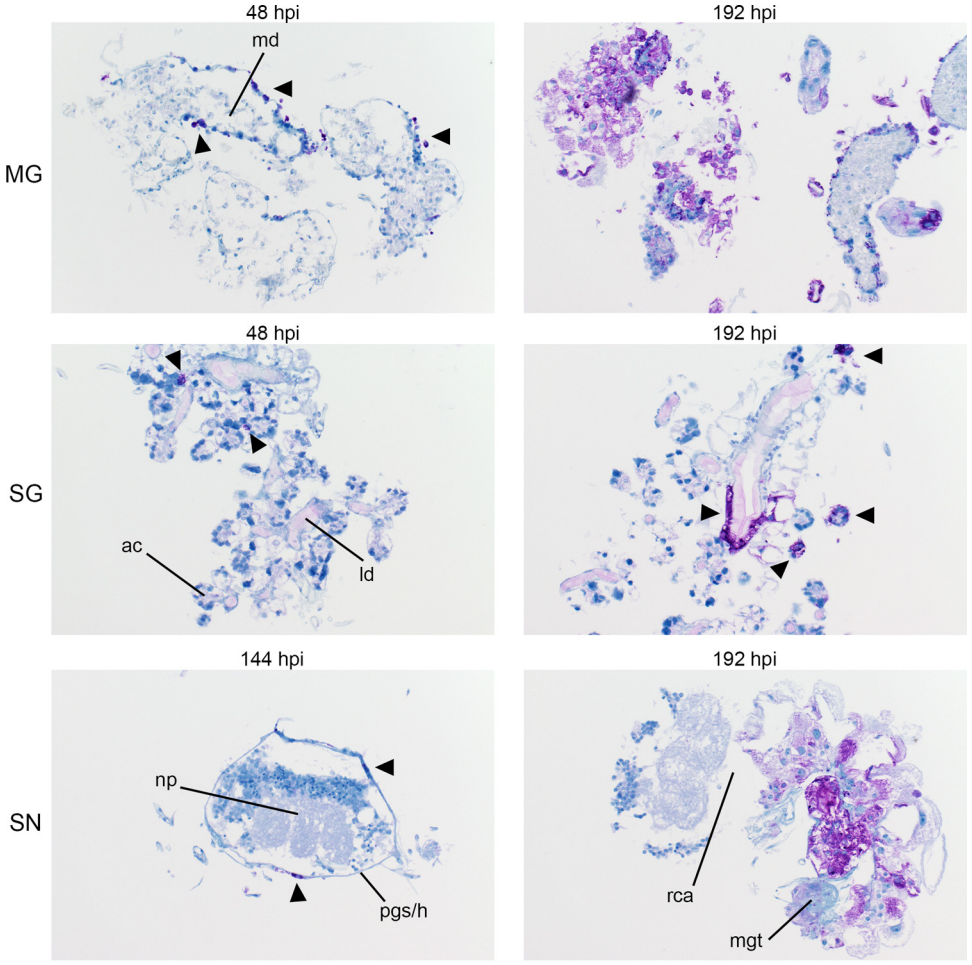

FIG 5 Progression of LGTV envelope protein synthesis in infected organ cultures. Magnification, ×20 (LGTV-infected MG, salivary gland [SG], and synganglion [SN]). md, midgut diverticulum; ld, lobular duct; a.c., acinus; pg/h, periganglionic sinus/sheath; n.p., neuropile; rca, retrocerebral area; mgt, midgut tissue. LGTV envelope protein within tissue is denoted by the prominent purple color. Mock-infected organs at 96 hpi were processed and stained in the same manner with LGTV antibody to identify any potential nonspecific staining background (see Fig. S3).

postinfection. At these collection time points, peak infectious LGTV and POWV production levels in the midgut cultures were observed at 108 hpi (Fig. 7A and 8A). Peak infectious LGTV and POWV levels in the salivary gland cultures were observed at 180 hpi (Fig. 7B and 8B). Similarly, peak infectious LGTV replication in the synganglion cultures was observed at 180 hpi (Fig. 7C), but infectious POWV replication did not peak during these time points (Fig. 8C). Taken together, these results provide evidence that short-term cultures of individual tick organs are sufficient for TBFV replication. In addition, greater levels of infectious LGTV replication, in comparison with infectious POWV replication, were observed from infected midguts at 36 to 180 hpi, from salivary glands at 108 to 180 hpi, and from synganglia at 180 hpi.

Reduction of infectious TBFV replication by dsRNA transfection targeting the LGTV 3′-UTR. In the previous sections, we demonstrated that dissected organs from female *I. scapularis* were viable in culture and that the cultures supported replication of the low-neurovirulence LGTV and the pathogenic POWV, thus indicating that the organ cultures were suitable for the detailed study of TBFV biology in a highly controlled arthropod system. The next aim in our long-term project was to examine the role of specific tick proteins in the various steps of the TBFV life cycle by targeting specific gene transcripts using dsRNA-mediated RNAi. The effect of transfecting dsRNA targeting transcripts of tick genes in organs as a way to disrupt TBFV replication has not been

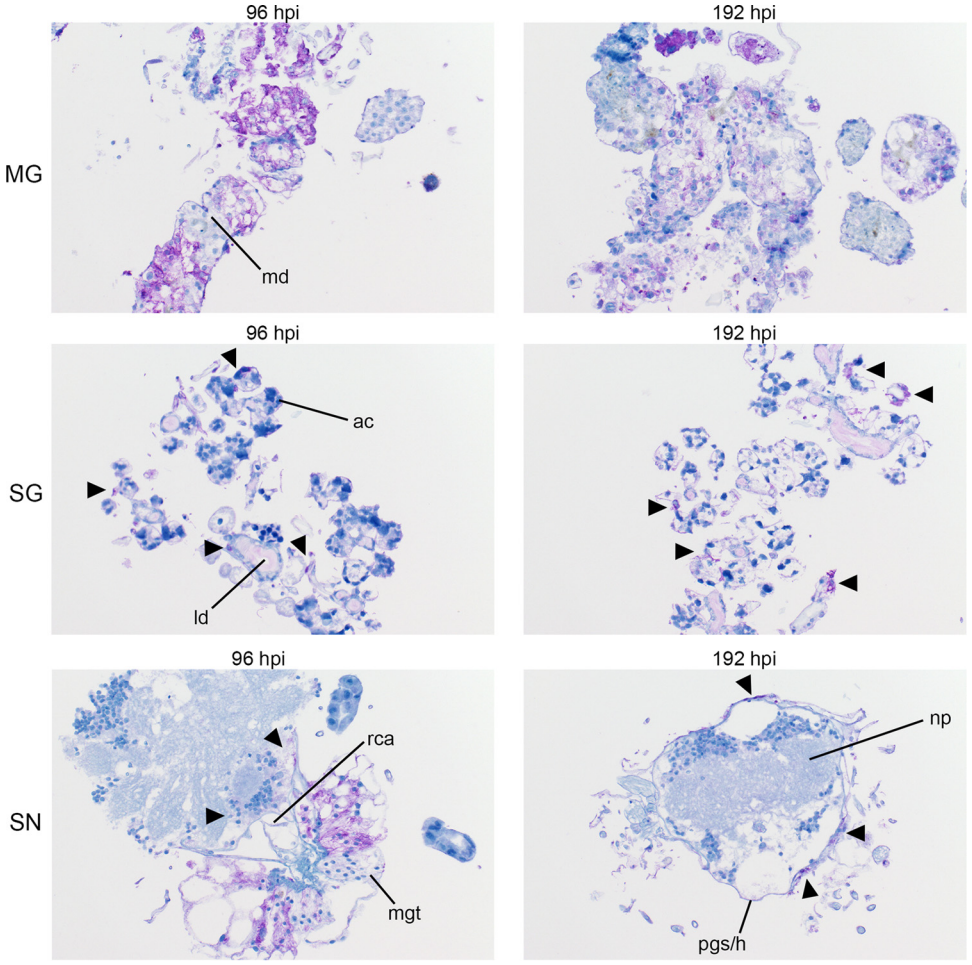

FIG 6 Progression of POWV protein synthesis in infected organ cultures. Magnification, ×20 (POWV-infected MG, salivary gland [SG], and synganglion [SN]). md, midgut diverticulum; ld, lobular duct; a.c., acinus; pg/h, perianglionic sinus/sheath; n.p., neuropile; rca, retrocerebral area; mgt, midgut tissue. POWV proteins within tissue are denoted by the prominent purple color. Mock-infected organs at 192 hpi were processed and stained in the same manner, using POWV antibody to identify any potential nonspecific staining background (see Fig. S3).

reported previously. As proof of principle, we targeted the 3′ UTR of the viral RNA with dsRNA, reasoning that if viral transcript knockdown was successful, virus replication would be impaired. Therefore, we transfected LGTV- and POWV-infected midguts and salivary glands with dsRNA targeting the LGTV 3′-UTR (48) and measured infectious virus at 108 and 180 hpi, respectively. Levels of infectious LGTV and POWV replication in both the midgut (Fig. 9A and B) and the salivary glands (Fig. 9C and D) were suppressed at least 10-fold (Fig. S4A to D). Importantly, LGTV 3′ UTR dsRNA transfection did not have a detrimental effect on organ viability (Fig. S5A and B). These results indicated that the tick organ cultures are a suitable system in which to study the effects of RNAi-mediated gene expression modification on TBFV replication.

DISCUSSION

The detailed study of virus biology in ticks has been hampered by a dearth of convenient systems. This is particularly true for work with highly pathogenic viruses, because arthropods infected with biosafety level 3 (BSL-3) or BSL-4 pathogens require laborious and cumbersome containment procedures during pathogenesis studies (62). Here, we have described methods that increase safety while investigating infection of arthropod tissues. Specifically, our study used dissected tick organs for *ex vivo* TBFV infection in order to (i) culture organs for periods of up to 9 to 10 days, (ii) assess the viability of individual organs while being cultured, (iii) dramatically reduce the handi-

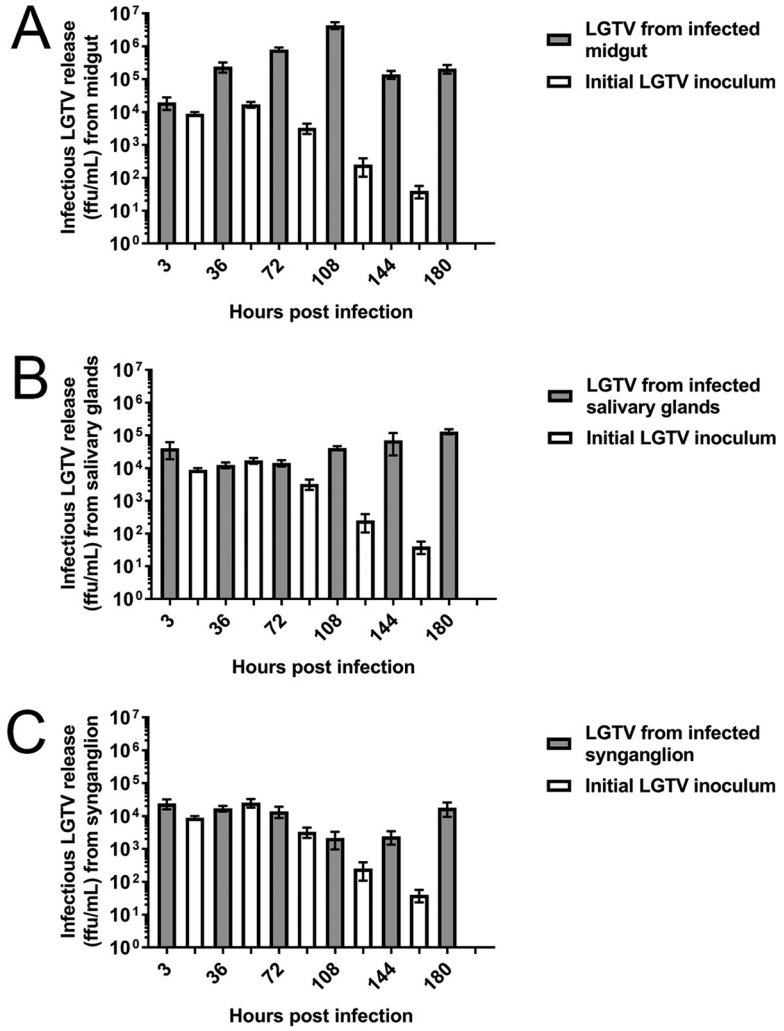

FIG 7 Infectious LGTV replication from infected organ cultures. Immunofocus assays were completed with supernatants collected from wells with LGTV-infected organs and control wells without organs (initial LGTV inoculum). Supernatants were collected from either one midgut (A), one salivary gland pair (B), or one synganglion (C) at each time point. Error bars represent standard errors of the means, and data are representative of two technical replicates for each sample for the immunofocus assays of two biological replicates.

caps of working with tick tissues infected with high-containment TBFV infection, and (iv) minimize the possibility of accidental sharps injuries during dissection of virus-infected ticks.

I. scapularis is a competent vector for both LGTV and POWV, and POWV specifically infects cells of midgut and salivary glands of the hard tick *D. andersoni* when infected *in vivo* (63). Based on these findings, we hypothesized that TBFVs would infect and replicate in *ex vivo I. scapularis* organs, even though the method deviated from the natural infection route *in vivo*. We found that both LGTV (Fig. 2, 3, 4, and 5; Fig. S1 and S2 and Movie S1 and S3) and POWV (Fig. 6; Fig. S1 and S2) infected midgut, salivary glands, and synganglion. Furthermore, there was clear evidence of virus spread in midgut (Fig. 2, 5, and 6; Movie S1 and S3) and salivary glands (Fig. 3, 5, and 6), but the evidence was uncertain in synganglion (Fig. 4, 5, and 6). Localization of both LGTV and POWV proteins in these organs was similar.

We used both LGTV^{GFP} localization and TBFV immunohistochemical staining of salivary glands (Fig. 3, 5, and 6; Fig. S2) to show that TBFV replication occurred both in the lobular ducts and in granular acini (acinus types II and/or III). Future confirmation and identification of the acinus type infected in this organ culture system by using

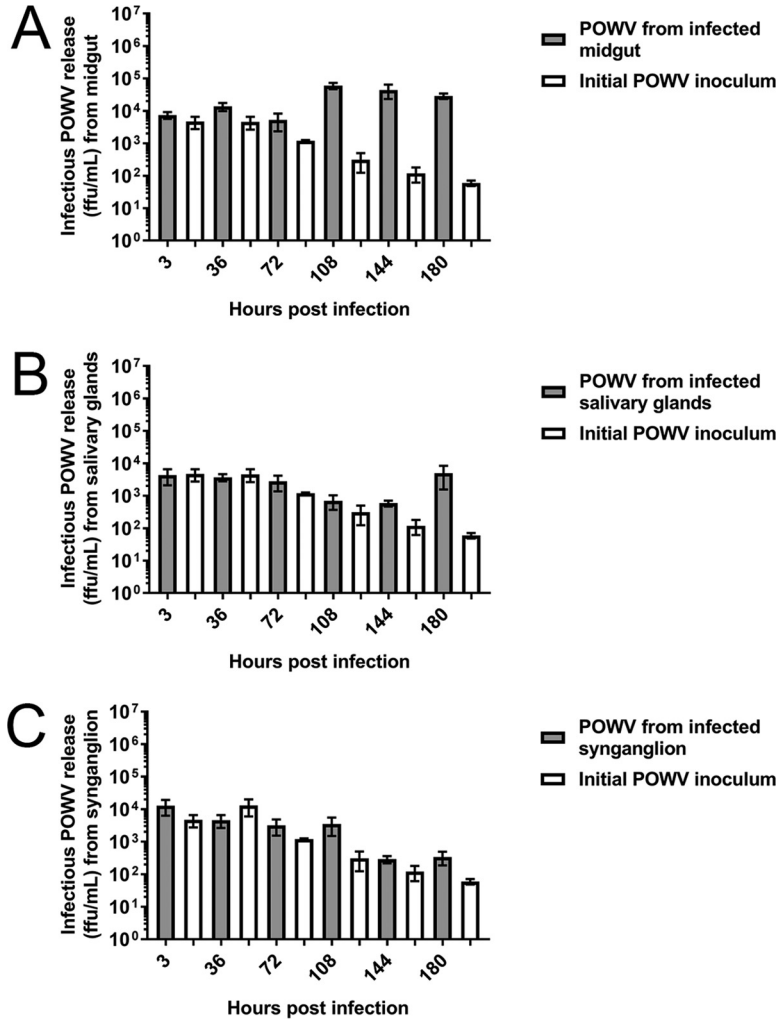

FIG 8 Infectious POWV replication from infected organ cultures. Immunofocus assays were completed with supernatants collected from wells with POWV-infected organs and control wells without organs (initial POWV inoculum). Supernatants were collected from either one midgut (A), one salivary gland pair (B), or one synganglion (C) at each time point. Error bars represent standard errors of the means, and data are representative of two technical replicates for each sample for immunofocus assays of two biological replicates.

electron and fluorescence microscopy may provide insight into how the virus is released into the saliva. It is known that TBFV transmission can occur within the first few hours of tick attachment (29, 64). This is likely due to the presence of virus in the salivary glands of unfed ticks and highlights the importance of tick salivary glands in POWV transmission. Furthermore, it is important to identify which type of acinus is susceptible to TBFV infection, since agranular (type I) and granular (type II and III) acini have distinct physiological functions (55, 56). As a result, the virus may be using and/or altering the function of the acini, and the pattern of secretion may differ between infected and uninfected acini (37). Future identification of protein expression and/or the secretome of TBFV-infected acini would be highly beneficial to provide insight into salivary gland biology in the context of TBFV transmission.

The synganglion typically serves as an organ of interest for tick control measures due to its neurological and motor control relevance. We were uncertain whether infectious LGTV or POWV replication measured from synganglion supernatants was produced from infected actual synganglion cell types or from the small part of the MGT that was attached following synganglion dissection (Fig. 4, 5, and 6; Table S1). However, LGTV^{GFP} was identified within the RCA of the synganglion (Fig. 4), and immunohisto-

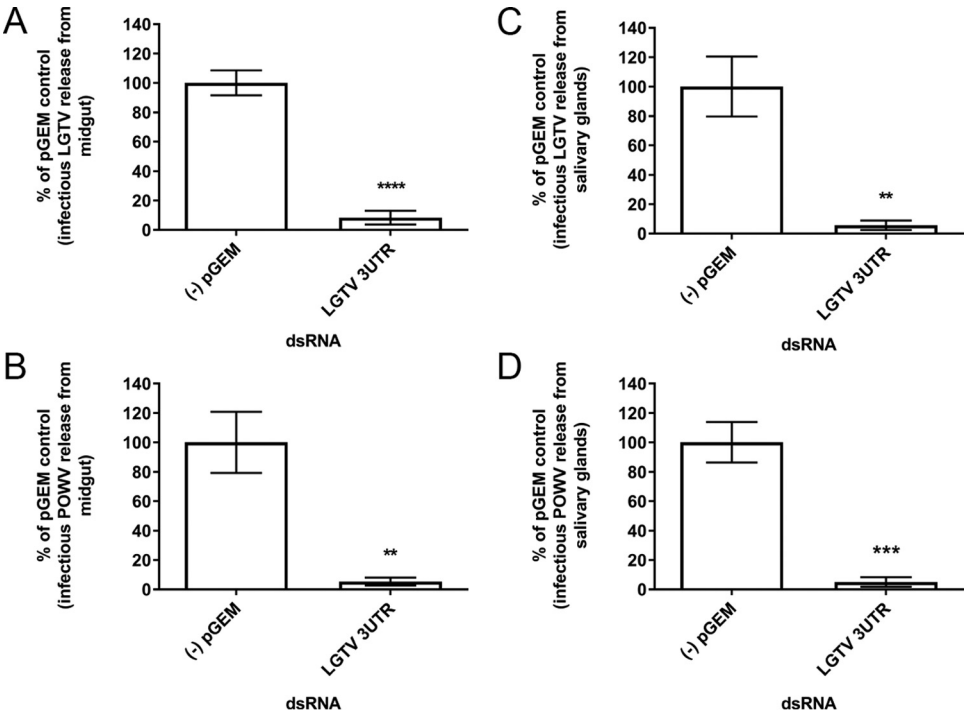

FIG 9 dsRNA transfection effect on infectious LGTV and POWV replication from infected midgut and salivary gland cultures. pGEM, pGEM plasmid (negative control); LGTV 3UTR, 3′ UTR of LGTV strain TP21. Transfection of LGTV-infected midgut (A), POWV-infected midgut (B), LGTV-infected salivary gland pair (C), and POWV-infected salivary gland pair (D) with 10 ng pGEM dsRNA and LGTV 3′ UTR dsRNA. Transfections of midguts and salivary glands were completed for 108 and 180 h, respectively, before supernatants were collected for immunofocus assays, which were normalized to the pGEM dsRNA negative-control response. An unpaired *t* test was completed to compare FFU per milliliter of the LGTV 3′ UTR dsRNA to that for the pGEM negative control. Error bars represent standard errors of the means, and data are representative of two technical replicates for each sample for the immunofocus assays of two biological replicates. **, $P \leq 0.01$; ***, $P \leq 0.001$; ****, $P \leq 0.0001$.

chemical staining showed LGTV (Fig. 5) and POWV (Fig. 6) proteins were found in the RCA and PGS/H of this organ. Thogoto virus, an orthomyxovirus, replicates within *Rhipicephalus appendiculatus* tick synganglion and in areas of the PGS/H as well (65). These findings suggest that certain viruses may have a tropism for the PGS/H in the tick synganglion. Possibly related is some evidence that TBFV infection in *Ixodes* spp. ticks is phenotypically associated with greater tick activity and aggression (35, 36), but the mechanisms for this behavior and whether it is associated with TBFV infection of the synganglion are unknown.

All three dissected organ types produced infectious LGTV (Fig. 7A to C) and POWV (Fig. 8A to C). Interestingly, all organ types produced at least 10-fold more infectious LGTV than POWV. These differences in infectious virus replication levels may reflect *I. scapularis* as a natural vector for POWV but not for LGTV. Also, POWV infections in this study were carried out with POWV lineage I, which may replicate differently than POWV lineage II (DTV) in *I. scapularis* organs. The latter virus has been isolated from naturally infected populations of *I. scapularis* (21, 22). Detailed growth comparisons between both POWV lineages in tick organ cultures may provide further insight. These findings suggest that the *ex vivo* organ culture system may also prove useful in examining genes responsible for arthropod host range determinants for specific tick species.

The development of new recombinant, live vaccine candidates against TBFVs would be facilitated by viruses with restricted replication. Incorporation of microRNA sequences into these vaccine candidates (66, 67) has provided a possible approach to increase the effectiveness of these live vaccines. Confirmation of restricted replication of these vaccine candidates in arthropod systems is also advisable. Thus, the *ex vivo* tick organ model offers a simplified screen for specific organs, such as the midgut and salivary glands.

Transfection of the LGTV 3′ UTR dsRNA in LGTV- and POWV-infected tick organs led to a decrease in not only infectious LGTV replication but also infectious POWV replication by at least 10-fold in both a midgut (Fig. S4A and B) and a salivary gland pair (Fig. S4C and D). This suggests that RNAi-mediated gene silencing is functional in the dissected, *I. scapularis* midgut and salivary glands, providing an RNAi-mediated antiviral response. Reduction of infectious POWV replication with LGTV 3′ UTR dsRNA transfection suggests that the nucleotide conservation of the 3′ UTR of both LGTV and POWV is high enough to stimulate a similar antiviral RNAi response corresponding to the POWV 3′ UTR. Little is known about endogenous dsRNA soaking of dissected *I. scapularis* midgut and salivary glands (44), although microinjection of *I. scapularis* with endogenous dsRNA (44, 68–73) provided successful transcript knockdown of endogenous gene expression. A proficient dsRNA-mediated transcript knockdown may also occur with *I. scapularis* organ culture; however, this is a subject that requires confirmation in future studies. Nonetheless, our study provides evidence that irrelevant pGEM and LGTV 3′ UTR dsRNA may be used for suitable negative and positive controls for future endogenous dsRNA transfection studies using LGTV- and POWV-infected *ex vivo* tick organs.

The genome of *I. scapularis* has been annotated (74–77), and *I. scapularis* transcripts have been targeted in many functional RNAi-mediated silencing studies. *I. scapularis* nymph transcript expression changes in association with TBFV infection have also been observed (37). In addition, hundreds of *I. scapularis* tick cell proteins have been identified to have expression changes in association with TBFV infection (47, 49). The identification of *I. scapularis* transcripts/proteins involved in TBFV infection needs to be explored *in vitro* and *in vivo*. Tick organ culture provides a convenient platform for these areas of investigation.

This study provides a foundation for using individual tick organs in cultures to study TBFV biology. However, variables exist that may affect organ viability and TBFV replication in organs, such as bloodfeeding and the virus concentration used for infection. Unfed female tick organs were utilized for this study (as in the study by Sunyakumthorn et al. [78]); thus, results may reflect a bias to a specific adult tick sex (or tick life stage) and physiological state. *In vivo* studies with TBEV in *Ixodes ricinus* ticks have shown higher levels of TBEV replication in blood-fed versus unfed ticks and, in particular, greater replication in salivary glands (60). We hypothesize that a similar trend may occur with TBFV replication in *ex vivo* organs from blood-fed versus unfed *I. scapularis* ticks; thus, use of organs from blood-fed ticks may be an option for future studies. In addition, different concentrations of the initial TBFV inoculum may also affect TBFV replication kinetics in these organs. Mitzel et al. showed that different concentrations for the LGTV inoculum affect the establishment of LGTV genome replication in *I. scapularis* larvae (30). Similarly, we suspect that different concentrations of the initial TBFV inoculum in female *I. scapularis* organ cultures could reveal varied levels of TBFV replication at different time points postinfection.

In summary, we have characterized the viability and extent of flavivirus infection of *I. scapularis ex vivo* organs, specifically showing a difference in replication between a low-neurovirulence flavivirus and a more pathogenic flavivirus. We highlighted cell types of specific tick organs that may be susceptible to flavivirus infection and utilized individual organs for dsRNA-mediated RNAi assays to show subsequent reductions in flavivirus replication. Overall, we have created a framework in which tick organ cultures can be utilized for further flavivirus pathogenesis studies using the tick system.

MATERIALS AND METHODS

***I. scapularis* tick organ dissection and preparation.** Unfed, female *I. scapularis* ticks were obtained from a laboratory colony maintained at the Oklahoma State University Tick Rearing Facility. Ticks were maintained as described by Mitzel et al. (30). Ticks were surface sterilized (79) by soaking them in 3% H_2O_2 for 15 s followed by soaking in 70% ethanol for 15 s. They were then wicked free of excess fluid on sterile Whatman paper and subsequently dissected in sterile phosphate-buffered saline (PBS) on a sterile glass microscope slide. The midgut was excised first and carefully removed from the cavity, followed by the salivary glands and synganglion. Tracheal tubes were removed carefully from the organs before experimental use. L15C-300 medium (80, 81) was used for organ culture and was not supplemented with antibiotics.

Organ viability assay. To determine the viability of dissected individual organs, separate organs were transferred, one at a time using one tip of the forceps, into complete L15C-300 medium with alamarBlue (a resazurin salt-based cell viability reagent; AbD Serotec, Raleigh, NC) at a 1:10 dilution in wells of a 96-well plate (49). The other tip of the forceps was dipped into a separate control well with medium supplemented the same way and served as a no-organ control.

Organs and their control wells were incubated at 34°C without CO_2 for 12 h, and absorbance was measured at a wavelength of 570 nm with a Molecular Devices SpectraMax Plus 384 plate reader and SoftMax Pro v6.5 software. Two machine replicates were completed with one organ per well and a corresponding control well that served as a biological replicate for each organ type. Three separate experiments were performed for each organ type ($n = 3$).

Cell and virus culture. *I. scapularis* ISE6 cells (kindly provided by Timothy Kurtti, University of Minnesota) were cultured at 34°C in complete L15C-300 medium without CO_2 (80, 81). Vero cells were cultured at 37°C in Dulbecco's modified Eagle's medium (Gibco, Life Technologies, Inc., Carlsbad, CA) supplemented with 10% fetal bovine serum (FBS; Gibco, Life Technologies, Inc., Carlsbad, CA) with 5% CO_2. LGTV and POWV stocks were created using African Green monkey kidney cells (Vero; ATCC). LGTV wild-type strain TP21, passage 5 stock was amplified in Vero cells (multiplicity of infection [MOI], 0.01) (82) and grown as described above, except with no FBS, to passage 6 in order to provide a working stock for experimental infections. POWV LB prototype strain (originally obtained from Robert Tesh, University of Texas Medical Branch) (83) stock was also amplified in Vero cells at the same MOI and grown in the same manner as LGTV to provide a working stock for experimental infections. LGTV and POWV stock titers were determined in immunofocus assays as described by Offerdahl et al. and Mlera et al. (57–59). The same method was used to determine infectious LGTV and POWV titers in experimental samples, with two technical replicates per sample. In parallel, a mock stock was prepared from mock-infected Vero cells.

LGTV^{GFP} plasmid construction. LGTV capable of enhanced GFP (eGFP) gene expression (LGTV^{GFP}) was generated using a strategy described previously (50). A PCR-amplified sequence of the eGFP gene was fused at the 3′ end with the codon-optimized sequence of the E/NS1 stem-anchor region (nucleotide positions 2171 to 2488 of the LGTV genome) of the RepC58 plasmid (66). This sequence was inserted into the infectious clone of the TP21 strain of LGTV (described by Tsetsarkin et al. [66]) at nucleotide position 2489 of the LGTV genome. The plasmid was propagated in *Escherichia coli* (strain MC1061) and purified using the Endo Free Plasmid Maxi kit (Qiagen, Valencia, CA). The sequence of the plasmid carrying the LGTV^{GFP} gene is available from the authors upon request.

Rescue of GFP-expressing LGTV. LGTV^{GFP} DNA plasmid transfection was carried out in Vero cells as described by Tsetsarkin et al. (66, 84), except that the X-tremeGene siRNA transfection reagent (Roche, Basel, Switzerland) was used per the manufacturer's instructions. Transfected cells were incubated for 7 days before supernatant was collected for infectious LGTV^{GFP} stock (LGTV^{GFP} passage 1). The titer for LGTV^{GFP} passage 1 stock was determined in immunofocus assays as described above with the LGTV TP21 strain stock. To create a mock stock for a control, supernatant was collected from transfected cells without the LGTV^{GFP} DNA plasmid and prepared in the same manner.

Virus infection of organs for LGTV^{GFP} expression, immunohistochemical staining, and infectious virus replication. LGTV^{GFP} infection of organs to image GFP expression was completed as follows. Organs were dissected as described above and placed into complete L15C-300 medium in an 8-well Labtek dish (Nunc, Rochester, NY). A total of 5×10^5 FFU of LGTV^{GFP} was placed into the infection wells, and mock stock was placed into the mock infection wells. One midgut, one salivary gland pair, and one synganglion were dissected and placed into separate LGTV^{GFP}-infected or mock-infected wells. One hour of adsorption with rocking at 34°C with no CO_2 was completed. Adsorption medium was carefully removed from the wells without removing the organs. Fresh complete L15C-300 medium was placed into the infection wells and cultures were incubated at 34°C with no CO_2. Serial imaging of LGTV^{GFP}-infected and mock-infected organs at 3, 36, 72, 108, 144, and 180 hpi was performed as described below.

To infect cultures with LGTV and POWV for immunohistochemical staining, organs were dissected as described above and placed into complete L15C-300 medium in wells of a 96-well plate. A total of 5×10^5 FFU of LGTV or POWV was placed into the infection wells, and mock stock was placed into mock infection wells. One hour of adsorption with rocking at 34°C with no CO_2 was completed. Infected organs were incubated at 34°C with no CO_2. Organs were collected at 48, 96, 144, and 192 hpi, with processing and staining of organs completed as described below.

LGTV and POWV infection of organs to determine levels of infectious virus replication were completed as follows. Sections (3 by 3 mm in size) of sterile gelfoam adsorbable gelatin sponge (Pharmacia and Upjohn, Kalamazoo, MI) were cut and submerged into complete L15C-300 medium in wells of a 96-well plate. Using sterile forceps, dissected organs were placed onto the soaked gelfoam and placed back into the original well. A total of 5×10^5 FFU of LGTV or POWV was placed into the well with the organ and into a well with no organ but just gelfoam (initial virus inoculum control; this control was used to separate the initial infectious virus inoculum from the infectious virus being produced from the organs). One hour of adsorption with rocking at 34°C with no CO_2 was completed. Adsorption medium was carefully removed without removing organs, and gelfoam with organs was carefully rinsed three times with sterile 1× PBS. After rinsing with PBS, complete L15C-300 medium was placed into each well, followed by incubation at 34°C with no CO_2. Wells with organs and control wells with no organs were processed in the same manner. Supernatants were collected from wells with organs and wells with no organs at 3, 36, 72, 108, 144, and 180 hpi, and virus titers were determined in immunofocus assays as described above, with two separate experiments for each organ type ($n = 2$).

Analysis of LGTV^{GFP} replication. LGTV^{GFP}-infected and mock-infected organs contained in the 8-well Labtek dish were viewed on a Zeiss model AxioVert.A1 microscope, and serial images and videos

of the LGTV^{GFP}-infected and mock-infected organs were captured using a Zeiss model AxioCam 503 mono camera. Fluorescence excitation was determined using the 89 North model PhotoFluor L.M. 75 images. Images and videos were processed with Zeiss ZEN 2 (Blue edition) software using autoexposure settings. Green fluorescent images and black and white videos were obtained with 10× magnification, with green and white denoting GFP expression in images and videos, respectively. Mock-infected organs were completed in parallel with LGTV^{GFP}-infected organs in order to identify potential autofluorescence that occurred with fluorescent imaging of tick organs (40, 63).

Paraffin processing and sectioning of dissected organs. Dissected tick organs consisting of midgut, salivary glands, and the synganglion that were infected with LGTV or POWV (as described above) for 48, 96, 144, and 192 hpi were fixed in 10% neutral buffered formalin (Cancer Diagnostics, Durham, NC) for a minimum of 24 h and then transferred to 70% ethanol. In parallel, mock-infected organs for 96 and 192 hpi were treated and collected in the same manner to provide negative controls for LGTV and POWV protein synthesis, respectively. Individual organs (midgut, salivary gland pair, or synganglion) were rinsed in PBS and covered in a thin layer of Histogel matrix (Thermo Scientific, Kalamazoo, MI). The Histogel matrix-encased organs were allowed to solidify at 4°C, placed in tissue cassettes, and processed using a VIP-6 Tissue Tek tissue system (Sakura Finetek, USA). Tick organs were embedded in Ultraffin paraffin polymer (Cancer Diagnostics, Durham, NC) and serially sectioned at 5 μm, and selected air-dried slides were stained with hematoxylin and eosin.

Immunohistochemical staining of viral proteins and imaging. Anti-POWV and anti-LGTV virus immunoreactivities were detected using POWV ascites fluid (which detects multiple viral proteins; ATCC) (59) at a 1:2,000 dilution and anti-LGTV-E mouse monoclonal antibody (detects viral E protein; 11H12) at a 1:50 dilution, respectively. The secondary antibody was a ready-to-use Discovery OmniMap anti-mouse horseradish peroxidase conjugate (prediluted; Roche). The tissues were then processed for immunohistochemical staining using the Discovery Ultra automated processor (Ventana Medical Systems, Tucson, AZ) with a Discovery Purple kit (Ventana Medical Systems). Stained cross-sections of infected and mock-infected organs were viewed on an Olympus model BX51 microscrope, and images were collected using an Olympus model DP80 camera. Images were processed with Olympus cellSens Dimension v1.13 software. Images were captured at 20×, 40×, and 100×magnification (indicated in the figures) with LGTV or POWV protein staining denoted by a prominent purple color. Mock-infected organs were processed in parallel with infected organs at 96 hpi with antibody for LGTV and at 192 hpi with antibody for POWV in order to identify any nonspecific staining.

Extraction of RNA from LGTV-infected ISE6 cells and cDNA synthesis. ISE6 cells grown to ~2 × 10^6 cells in a T25 flask were infected with LGTV at an MOI of 10. After 36 hpi, medium was removed and RLT lysis buffer (from the Qiagen RNeasy minikit) was directly applied to lyse the attached cells. Further processing of LGTV-infected ISE6 RNA was carried out according to the manufacturer's instructions for the RNeasy minikit (Qiagen).

An iScript cDNA synthesis kit (Bio-Rad, Hercules, CA) and corresponding instructions were used to synthesize cDNA from RNA samples. The following thermocycler conditions were used for cDNA synthesis: 25°C for 5 min, 42°C for 50 min, and 85°C for 5 min (48).

Synthesis of dsRNA. A pGEM-T Easy vector DNA plasmid (Promega, Madison, WI) with the forward primer 5′-TAATACGACTCACTATAGGGGGTATCAGCTCACTCAAAGG-3′ and reverse primer 5′-TAATACGACTCACTATAGGGGAACGACCTACACCGAACT-3′ were used to generate the pGEM T7-tagged DNA. cDNA synthesized from LGTV-infected ISE6 RNA with forward primer 5′-TAATACGACTCACTATAGGGCCAGACACAAGGAGTCCAA-3′ and reverse primer 5′-TAATACGACTCACTATAGGGATGGTGGCTCAGGGAGAAC-3′) were used to generate the LGTV 3′ UTR T7-tagged cDNA template (48). The following two-step PCR thermocycler conditions were used to amplify T7-tagged pGEM DNA and LGTV 3′ UTR cDNA: 94°C for 5 min; 5 cycles at 94°C for 30 s, 58°C for 30 s, and 72°C for 2 min; 27 cycles at 94°C for 30 s, 68°C for 30 s, and 72°C for 2 min, and a final extension at 72°C for 7 min. This amplified T7-tagged pGEM DNA and LGTV 3′ UTR cDNA were used to synthesize dsRNA with the MEGAscript RNAi synthesis kit (Ambion, Waltham, MA) according to the kit instructions and procedures used in previous studies (48, 85).

Transfection of infected tick organs with dsRNA. LGTV and POWV infection and incubation of midgut and salivary glands for posttreatment with pGEM or LGTV 3′ UTR dsRNA were completed as described above for infecting organs to determine infectious virus replication, except 100 μl complete L15C-300 medium was placed into each well followed by 50 μl dsRNA transfection mix prepared according to methods described in references 48 and 85 with 10 ng dsRNA (150-μl total volume in the well). With the used initial virus inoculum concentration (5× 10^5 FFU), midgut and salivary glands were transfected for 108 and 180 h, respectively, since peak infectious LGTV and POWV replication levels were observed for the midgut and salivary glands at these time points. Supernatants were collected from these infected, dsRNA-transfected organs and subjected to immunofocus assays (as described above) to determine infectious virus replication levels.

The effects of LGTV 3′ UTR dsRNA transfection on midgut and salivary gland viability were assessed as described above for transfecting organs, except organs were not infected and were placed directly into 96 wells with the transfection-medium mix with no gelfoam. After the specified transfection time, midgut and salivary glands were removed and placed into alamarBlue-infused medium. Organs were incubated for 12 h, and viability readings were collected as described above.

SUPPLEMENTAL MATERIAL

Supplemental material for this article may be found at https://doi.org/10.1128/mBio.01255-17.

FIG S1, JPG file, 1.6 MB.

FIG S2, JPG file, 1.6 MB.
FIG S3, JPG file, 2.6 MB.
FIG S4, TIF file, 0.1 MB.
FIG S5, TIF file, 0.2 MB.
TABLE S1, DOCX file, 0.01 MB.
MOVIE S1, MPG file, 14.6 MB.
MOVIE S2, MPG file, 14.6 MB.
MOVIE S3, MPG file, 19.1 MB.
MOVIE S4, MPG file, 19.3 MB.

ACKNOWLEDGMENTS

We thank Chad Hillman (LZP/NIAID/NIH, Hamilton, MT) and Patricia Rosa (LZP/NIAID/NIH, Hamilton, MT) for providing the dissecting scope used for tick dissection, Tina Thomas (DMT/NIAID/NIH, Hamilton, MT) for aid in histology experimental work, and Austin Athman, Ryan Kissinger, and Anita Mora of the Visual Medical Arts of the Research and Technologies Branch (NIAID/NIH, Hamilton, MT) for graphic art. We appreciate the early evaluation of the manuscript by Libor Grubhoffer (Czech Academy of Sciences/University of South Bohemia).

This research was supported by the Intramural Research Program of the National Institute of Allergy and Infectious Diseases of the National Institutes of Health.

REFERENCES

1. Dantas-Torres F, Chomel BB, Otranto D. 2012. Ticks and tick-borne diseases: a One Health perspective. Trends Parasitol 28:437–446. https://doi.org/10.1016/j.pt.2012.07.003.
2. Jongejan F, Uilenberg G. 2004. The global importance of ticks. Parasitology 129(Suppl):S3–S14. https://doi.org/10.1017/S0031182004005967.
3. Piesman J, Eisen L. 2008. Prevention of tick-borne diseases. Annu Rev Entomol 53:323–343. https://doi.org/10.1146/annurev.ento.53.103106.093429.
4. Cutler SJ. 2010. Relapsing fever—a forgotten disease revealed. J Appl Microbiol 108:1115–1122. https://doi.org/10.1111/j.1365-2672.2009.04598.x.
5. Breitschwerdt EB, Hegarty BC, Maggi RG, Lantos PM, Aslett DM, Bradley JM. 2011. *Rickettsia rickettsii* transmission by a lone star tick, North Carolina. Emerg Infect Dis 17:873–875. https://doi.org/10.3201/eid1705.101530.
6. Gyuranecz M, Rigó K, Dán A, Földvári G, Makrai L, Dénes B, Fodor L, Majoros G, Tirják L, Erdélyi K. 2011. Investigation of the ecology of *Francisella tularensis* during an inter-epizootic period. Vector Borne Zoonotic Dis 11:1031–1035. https://doi.org/10.1089/vbz.2010.0091.
7. Dobler G. 2010. Zoonotic tick-borne flaviviruses. Vet Microbiol 140:221–228. https://doi.org/10.1016/j.vetmic.2009.08.024.
8. Lasala PR, Holbrook M. 2010. Tick-borne flaviviruses. Clin Lab Med 30:221–235. https://doi.org/10.1016/j.cll.2010.01.002.
9. Gritsun TS, Nuttall PA, Gould EA. 2003. Tick-borne flaviviruses. Adv Virus Res 61:317–371. https://doi.org/10.1016/S0065-3527(03)61008-0.
10. Pletnev AG, Men R. 1998. Attenuation of the Langat tick-borne flavivirus by chimerization with mosquito-borne flavivirus dengue type 4. Proc Natl Acad Sci U S A 95:1746–1751. https://doi.org/10.1073/pnas.95.4.1746.
11. Maffioli C, Grandgirard D, Leib SL, Engler O. 2012. siRNA inhibits replication of Langat virus, a member of the tick-borne encephalitis virus complex in organotypic rat brain slices. PLoS One 7:e44703. https://doi.org/10.1371/journal.pone.0044703.
12. Price WH, Thind IS, Teasdall RD, O'Leary W. 1970. Vaccination of human volunteers against Russian spring-summer (RSS) virus complex with attenuated Langat E5 virus. Bull World Health Organ 42:89–94.
13. Smith CE. 1956. A virus resembling Russian spring-summer encephalitis virus from an ixodid tick in Malaya. Nature 178:581–582. https://doi.org/10.1038/178581a0.
14. Lindquist L, Vapalahti O. 2008. Tick-borne encephalitis. Lancet 371:1861–1871. https://doi.org/10.1016/S0140-6736(08)60800-4.
15. Ebel GD. 2010. Update on Powassan virus: emergence of a North American tick-borne flavivirus. Annu Rev Entomol 55:95–110. https://doi.org/10.1146/annurev-ento-112408-085446.
16. Ebel GD, Spielman A, Telford SR, III. 2001. Phylogeny of North American Powassan virus. J Gen Virol 82:1657–1665. https://doi.org/10.1099/0022-1317-82-7-1657.
17. Kuno G, Artsob H, Karabatsos N, Tsuchiya KR, Chang GJ. 2001. Genomic sequencing of deer tick virus and phylogeny of Powassan-related viruses of North America. Am J Trop Med Hyg 65:671–676. https://doi.org/10.4269/ajtmh.2001.65.671.
18. Hinten SR, Beckett GA, Gensheimer KF, Pritchard E, Courtney TM, Sears SD, Woytowicz JM, Preston DG, Smith RP, Jr, Rand PW, Lacombe EH, Holman MS, Lubelczyk CB, Kelso PT, Beelen AP, Stobierski MG, Sotir MJ, Wong S, Ebel G, Kosoy O, Piesman J, Campbell GL, Marfin AA. 2008. Increased recognition of Powassan encephalitis in the United States, 1999–2005. Vector Borne Zoonotic Dis 8:733–740. https://doi.org/10.1089/vbz.2008.0022.
19. National Academies of Sciences, Engineering, and Medicine. 2016. Global health impacts of vector-borne diseases: workshop summary. National Academies Press, Washington, DC.
20. Brackney DE, Nofchissey RA, Fitzpatrick KA, Brown IK, Ebel GD. 2008. Stable prevalence of Powassan virus in *Ixodes scapularis* in a northern Wisconsin focus. Am J Trop Med Hyg 79:971–973.
21. Aliota MT, Dupuis AP, II, Wilczek MP, Peters RJ, Ostfeld RS, Kramer LD. 2014. The prevalence of zoonotic tick-borne pathogens in *Ixodes scapularis* collected in the Hudson Valley, New York State. Vector Borne Zoonotic Dis 14:245–250. https://doi.org/10.1089/vbz.2013.1475.
22. Dupuis AP, II, Peters RJ, Prusinski MA, Falco RC, Ostfeld RS, Kramer LD. 2013. Isolation of deer tick virus (Powassan virus, lineage II) from *Ixodes scapularis* and detection of antibody in vertebrate hosts sampled in the Hudson Valley, New York State. Parasit Vectors 6:185. https://doi.org/10.1186/1756-3305-6-185.
23. Main AJ, Carey AB, Downs WG. 1979. Powassan virus in *Ixodes cookei* and Mustelidae in New England. J Wildl Dis 15:585–591. https://doi.org/10.7589/0090-3558-15.4.585.
24. McLean DM, Best JM, Mahalingam S, Chernesky MA, Wilson WE. 1964. Powassan virus: summer infection cycle, 1964. Can Med Assoc J 91:1360–1362.
25. McLean DM, Larke RP. 1963. Powassan and Silverwater viruses: ecology of two Ontario arboviruses. Can Med Assoc J 88:182–185.
26. Thomas LA, Kennedy RC, Eklund CM. 1960. Isolation of a virus closely related to Powassan virus from *Dermacentor andersoni* collected along North Caché la Poudre River, Colo. Proc Soc Exp Biol Med 104:355–359. https://doi.org/10.3181/00379727-104-25836.
27. Costero A, Grayson MA. 1996. Experimental transmission of Powassan virus (Flaviviridae) by *Ixodes scapularis* ticks (Acari:Ixodidae). Am J Trop Med Hyg 55:536–546. https://doi.org/10.4269/ajtmh.1996.55.536.

28. Chernesky MA. 1969. Powassan virus transmission by ixodid ticks infected after feeding on viremic rabbits injected intravenously. Can J Microbiol 15:521–526. https://doi.org/10.1139/m69-090.
29. Ebel GD, Kramer LD. 2004. Short report: duration of tick attachment required for transmission of powassan virus by deer ticks. Am J Trop Med Hyg 71:268–271.
30. Mitzel DN, Wolfinbarger JB, Long RD, Masnick M, Best SM, Bloom ME. 2007. Tick-borne flavivirus infection in *Ixodes scapularis* larvae: development of a novel method for synchronous viral infection of ticks. Virology 365:410–418. https://doi.org/10.1016/j.virol.2007.03.057.
31. Nuttall PA, Labuda M. 2003. Dynamics of infection in tick vectors and at the tick-host interface. Adv Virus Res 60:233–272. https://doi.org/10.1016/S0065-3527(03)60007-2.
32. Nuttall PA, Jones LD, Davies CR. 1991. The role of arthropod vectors in arbovirus evolution, p 15–45. *In* Harris KF (ed), Advances in disease vector research. Springer, New York, NY.
33. Bell-Sakyi L, Zweygarth E, Blouin EF, Gould EA, Jongejan F. 2007. Tick cell lines: tools for tick and tick-borne disease research. Trends Parasitol 23:450–457. https://doi.org/10.1016/j.pt.2007.07.009.
34. Bell-Sakyi L, Kohl A, Bente DA, Fazakerley JK. 2012. Tick cell lines for study of Crimean-Congo hemorrhagic fever virus and other arboviruses. Vector Borne Zoonotic Dis 12:769–781. https://doi.org/10.1089/vbz.2011.0766.
35. Alekseev AN, Burenkova LA, Chunikhin SP. 1988. Behavioral characteristics of *Ixodes persulcatus* P. Sch. ticks infected with the tick-borne encephalitis virus. Med Parazitol (Mosk) 71–75. (In Russian.)
36. Belova OA, Burenkova LA, Karganova GG. 2012. Different tick-borne encephalitis virus (TBEV) prevalences in unfed versus partially engorged ixodid ticks—evidence of virus replication and changes in tick behavior. Ticks Tick Borne Dis 3:240–246. https://doi.org/10.1016/j.ttbdis.2012.05.005.
37. McNally KL, Mitzel DN, Anderson JM, Ribeiro JM, Valenzuela JG, Myers TG, Godinez A, Wolfinbarger JB, Best SM, Bloom ME. 2012. Differential salivary gland transcript expression profile in *Ixodes scapularis* nymphs upon feeding or flavivirus infection. Ticks Tick Borne Dis 3:18–26. https://doi.org/10.1016/j.ttbdis.2011.09.003.
38. Khozinskaya GA, Chunikhin SP, Khozinsky VV, Stefutkina LF. 1985. Variability of Powassan virus cultured in tissue explants and organism of *Hyalomma anatolicum* ticks. Acta Virol 29:305–311.
39. Chunikhin SP, Khozinskaia GA, Stefutkina LF, Korolev MB. 1984. Mono- and mixed infection by the tick-borne encephalitis and Powassan viruses of tissue explants from ticks of the genus *Hyalomma*. Parazitologiia 18:116–122.
40. Bell-Sakyi L, Weisheit S, Rückert C, Barry G, Fazakerley J, Fragkoudis R. 2016. Microscopic visualisation of zoonotic arbovirus replication in tick cell and organ cultures using Semliki Forest virus reporter systems. Vet Sci 3:28. https://doi.org/10.3390/vetsci3040028.
41. Karim S, Miller NJ, Valenzuela J, Sauer JR, Mather TN. 2005. RNAi-mediated gene silencing to assess the role of synaptobrevin and cystatin in tick blood feeding. Biochem Biophys Res Commun 334:1336–1342. https://doi.org/10.1016/j.bbrc.2005.07.036.
42. Aljamali MN, Bior AD, Sauer JR, Essenberg RC. 2003. RNA interference in ticks: a study using histamine binding protein dsRNA in the female tick *Amblyomma americanum*. Insect Mol Biol 12:299–305. https://doi.org/10.1046/j.1365-2583.2003.00416.x.
43. Karim S, Ramakrishnan VG, Tucker JS, Essenberg RC, Sauer JR. 2004. *Amblyomma americanum* salivary glands: double-stranded RNA-mediated gene silencing of synaptobrevin homologue and inhibition of PGE2 stimulated protein secretion. Insect Biochem Mol Biol 34:407–413. https://doi.org/10.1016/j.ibmb.2004.01.005.
44. de la Fuente J, Kocan KM, Almazán C, Blouin EF. 2007. RNA interference for the study and genetic manipulation of ticks. Trends Parasitol 23:427–433. https://doi.org/10.1016/j.pt.2007.07.002.
45. Ramakrishnan VG, Aljamali MN, Sauer JR, Essenberg RC. 2005. Application of RNA interference in tick salivary gland research. J Biomol Tech 16:297–305.
46. Schnettler E, Tykalová H, Watson M, Sharma M, Sterken MG, Obbard DJ, Lewis SH, McFarlane M, Bell-Sakyi L, Barry G, Weisheit S, Best SM, Kuhn RJ, Pijlman GP, Chase-Topping ME, Gould EA, Grubhoffer L, Fazakerley JK, Kohl A. 2014. Induction and suppression of tick cell antiviral RNAi responses by tick-borne flaviviruses. Nucleic Acids Res 42:9436–9446. https://doi.org/10.1093/nar/gku657.
47. Weisheit S, Villar M, Tykalová H, Popara M, Loecherbach J, Watson M, Růžek D, Grubhoffer L, de la Fuente J, Fazakerley JK, Bell-Sakyi L. 2015. *Ixodes scapularis* and *Ixodes ricinus* tick cell lines respond to infection with tick-borne encephalitis virus: transcriptomic and proteomic analysis. Parasit Vectors 8:599. https://doi.org/10.1186/s13071-015-1210-x.
48. Grabowski JM, Gulia-Nuss M, Kuhn RJ, Hill CA. 2017. RNAi reveals proteins for metabolism and protein processing associated with Langat virus infection in *Ixodes scapularis* (black-legged tick) ISE6 cells. Parasit Vectors 10:24. https://doi.org/10.1186/s13071-016-1944-0.
49. Grabowski JM, Perera R, Roumani AM, Hedrick VE, Inerowicz HD, Hill CA, Kuhn RJ. 2016. Changes in the proteome of Langat-infected *Ixodes scapularis* ISE6 cells: metabolic pathways associated with flavivirus infection. PLoS Negl Trop Dis 10:e0004180. https://doi.org/10.1371/journal.pntd.0004180.
50. Bonaldo MC, Mello SM, Trindade GF, Rangel AA, Duarte AS, Oliveira PJ, Freire MS, Kubelka CF, Galler R. 2007. Construction and characterization of recombinant flaviviruses bearing insertions between E and NS1 genes. Virol J 4:115. https://doi.org/10.1186/1743-422X-4-115.
51. de Santana MG, Neves PC, dos Santos JR, Lima NS, dos Santos AA, Watkins DI, Galler R, Bonaldo MC. 2014. Improved genetic stability of recombinant yellow fever 17D virus expressing a lentiviral Gag gene fragment. Virology 452–453:202–211. https://doi.org/10.1016/j.virol.2014.01.017.
52. Sonenshine DE, Anderson JM. 2014. Mouthparts and digestive system: anatomy and molecular biology of feeding and digestion, p 122–162. *In* Sonenshine DE, Roe RM (ed), Biology of ticks, vol. 1. Oxford University Press, Bethesda, MD.
53. Raikhel AS. 1983. The intestine, p 59–97. *In* Balashov YS, Raikhel AS, Hoogstraal H (ed), An atlas of ixodid tick ultrastructure. Entomological Society of America, Annapolis, MD.
54. Balashov YS. 1983. Salivary glands, p 98–128. *In* Balashov YS, Raikhel AS, Hoogstraal H (ed), An atlas of ixodid tick ultrastructure. Entomological Society of America, Annapolis, MD.
55. Bowman AS, Ball A, Sauer JR. 2008. Tick salivary glands: the physiology of tick water balance and their role in pathogen trafficking and transmission, p 73–91. *In* Bowman AS, Nuttall P (ed), Ticks: biology, disease and control. Cambridge University Press, New York, NY.
56. Alarcon-Chaidez FJ. 2014. Salivary glands: structure, physiology, and molecular biology, p 163–205. *In* Sonenshine DE, Roe RM (ed), Biology of ticks, vol. 1, 2nd ed. Oxford University Press, Bethesda, MD.
57. Mlera L, Offerdahl DK, Martens C, Porcella SF, Melik W, Bloom ME. 2015. Development of a model system for tick-borne flavivirus persistence in HEK 293T Cells. mBio 6:e00614-15. https://doi.org/10.1128/mBio.00614-15.
58. Mlera L, Lam J, Offerdahl DK, Martens C, Sturdevant D, Turner CV, Porcella SF, Bloom ME. 2016. Transcriptome analysis reveals a signature profile for tick-borne Flavivirus persistence in HEK 293T Cells. mBio 7:e00314-16. https://doi.org/10.1128/mBio.00314-16.
59. Offerdahl DK, Dorward DW, Hansen BT, Bloom ME. 2012. A three-dimensional comparison of tick-borne flavivirus infection in mammalian and tick cell lines. PLoS One 7:e47912. https://doi.org/10.1371/journal.pone.0047912.
60. Slovák M, Kazimírová M, Siebenstichová M, Ustaníková K, Klempa B, Gritsun T, Gould EA, Nuttall PA. 2014. Survival dynamics of tick-borne encephalitis virus in *Ixodes ricinus* ticks. Ticks Tick Borne Dis 5:962–969. https://doi.org/10.1016/j.ttbdis.2014.07.019.
61. Khasnatinov MA, Ustanikova K, Frolova TV, Pogodina VV, Bochkova NG, Levina LS, Slovak M, Kazimirova M, Labuda M, Klempa B, Eleckova E, Gould EA, Gritsun TS. 2009. Non-hemagglutinating flaviviruses: molecular mechanisms for the emergence of new strains via adaptation to European ticks. PLoS One 4:e7295. https://doi.org/10.1371/journal.pone.0007295.
62. American Committee of Medical Entomology, American Society of Tropical Medicine and Hygiene. 2003. Arthropod containment guidelines. A project of the American Committee of Medical Entomology and American Society of Tropical Medicine and Hygiene. Vector Borne Zoonotic Dis 3:61–98. https://doi.org/10.1089/153036603322163448.
63. Chernesky MA, McLean DM. 1969. Localization of Powassan virus in *Dermacentor andersoni* ticks by immunofluorescence. Can J Microbiol 15:1399–1408. https://doi.org/10.1139/m69-252.
64. Hermance ME, Thangamani S. 2014. Proinflammatory cytokines and chemokines at the skin interface during Powassan virus transmission. J Invest Dermatol 134:2280–2283. https://doi.org/10.1038/jid.2014.150.
65. Booth TF, Davies CR, Jones LD, Staunton D, Nuttall PA. 1989. Anatomical basis of Thogoto virus infection in BHK cell culture and in the ixodid tick vector, *Rhipicephalus appendiculatus*. J Gen Virol 70:1093–1104. https://doi.org/10.1099/0022-1317-70-5-1093.

66. Tsetsarkin KA, Liu G, Kenney H, Hermance M, Thangamani S, Pletnev AG. 2016. Concurrent micro-RNA mediated silencing of tick-borne flavivirus replication in tick vector and in the brain of vertebrate host. Sci Rep 6:33088. https://doi.org/10.1038/srep33088.
67. Tsetsarkin KA, Liu G, Volkova E, Pletnev AG. 2017. Synergistic internal ribosome entry site/microRNA-based approach for flavivirus attenuation and live vaccine development. mBio 8:e02326-16. https://doi.org/10.1128/mBio.02326-16.
68. de la Fuente J, Almazán C, Blouin EF, Naranjo V, Kocan KM. 2005. RNA interference screening in ticks for identification of protective antigens. Parasitol Res 96:137–141. https://doi.org/10.1007/s00436-005-1351-5.
69. Narasimhan S, Montgomery RR, DePonte K, Tschudi C, Marcantonio N, Anderson JF, Sauer JR, Cappello M, Kantor FS, Fikrig E. 2004. Disruption of *Ixodes scapularis* anticoagulation by using RNA interference. Proc Natl Acad Sci U S A 101:1141–1146. https://doi.org/10.1073/pnas.0307669100.
70. Pal U, Li X, Wang T, Montgomery RR, Ramamoorthi N, Desilva AM, Bao F, Yang X, Pypaert M, Pradhan D, Kantor FS, Telford S, Anderson JF, Fikrig E. 2004. TROSPA, an *Ixodes scapularis* receptor for *Borrelia burgdorferi*. Cell 119:457–468. https://doi.org/10.1016/j.cell.2004.10.027.
71. Ramamoorthi N, Narasimhan S, Pal U, Bao F, Yang XF, Fish D, Anguita J, Norgard MV, Kantor FS, Anderson JF, Koski RA, Fikrig E. 2005. The Lyme disease agent exploits a tick protein to infect the mammalian host. Nature 436:573–577. https://doi.org/10.1038/nature03812.
72. Sukumaran B, Narasimhan S, Anderson JF, DePonte K, Marcantonio N, Krishnan MN, Fish D, Telford SR, Kantor FS, Fikrig E. 2006. An *Ixodes scapularis* protein required for survival of *Anaplasma phagocytophilum* in tick salivary glands. J Exp Med 203:1507–1517. https://doi.org/10.1084/jem.20060208.
73. Pedra JH, Narasimhan S, Deponte K, Marcantonio N, Kantor FS, Fikrig E. 2006. Disruption of the salivary protein 14 in *Ixodes scapularis* nymphs and impact on pathogen acquisition. Am J Trop Med Hyg 75:677–682.
74. Gulia-Nuss M, Nuss AB, Meyer JM, Sonenshine DE, Roe RM, Waterhouse RM, Sattelle DB, de la Fuente J, Ribeiro JM, Megy K, Thimmapuram J, Miller JR, Walenz BP, Koren S, Hostetler JB, Thiagarajan M, Joardar VS, Hannick LI, Bidwell S, Hammond MP, Young S, Zeng Q, Abrudan JL, Almeida FC, Ayllón N, Bhide K, Bissinger BW, Bonzon-Kulichenko E, Buckingham SD, Caffrey DR, Caimano MJ, Croset V, Driscoll T, Gilbert D, Gillespie JJ, Giraldo-Calderón GI, Grabowski JM, Jiang D, Khalil SM, Kim D, Kocan KM, Koci J, Kuhn RJ, Kurtti TJ, Lees K, Lang EG, Kennedy RC, Kwon H, Perera R, Qi Y, et al. 2016. Genomic insights into the *Ixodes scapularis* tick vector of Lyme disease. Nat Commun 7:10507. https://doi.org/10.1038/ncomms10507.
75. de la Fuente J, Waterhouse RM, Sonenshine DE, Roe RM, Ribeiro JM, Sattelle DB, Hill CA. 2016. Tick genome assembled: new opportunities for research on tick-host-pathogen interactions. Front Cell Infect Microbiol 6:103. https://doi.org/10.3389/fcimb.2016.00103.
76. Hill CA, Wikel SK. 2005. The *Ixodes scapularis* genome project: an opportunity for advancing tick research. Trends Parasitol 21:151–153. https://doi.org/10.1016/j.pt.2005.02.004.
77. Pagel Van Zee J, Geraci NS, Guerrero FD, Wikel SK, Stuart JJ, Nene VM, Hill CA. 2007. Tick genomics: the *Ixodes* genome project and beyond. Int J Parasitol 37:1297–1305. https://doi.org/10.1016/j.ijpara.2007.05.011.
78. Sunyakumthorn P, Petchampai N, Grasperge BJ, Kearney MT, Sonenshine DE, Macaluso KR. 2013. Gene expression of tissue-specific molecules in *ex vivo Dermacentor variabilis* (Acari: Ixodidae) during rickettsial exposure. J Med Entomol 50:1089–1096. https://doi.org/10.1603/ME12162.
79. Patton TG, Dietrich G, Brandt K, Dolan MC, Piesman J, Gilmore RD, Jr. 2012. Saliva, salivary gland, and hemolymph collection from *Ixodes scapularis* ticks. J Vis Exp https://doi.org/10.3791/3894.
80. Munderloh UG, Kurtti TJ. 1989. Formulation of medium for tick cell culture. Exp Appl Acarol 7:219–229. https://doi.org/10.1007/BF01194061.
81. Munderloh UG, Liu Y, Wang M, Chen C, Kurtti TJ. 1994. Establishment, maintenance and description of cell lines from the tick *Ixodes scapularis*. J Parasitol 80:533–543. https://doi.org/10.2307/3283188.
82. Campbell MS, Pletnev AG. 2000. Infectious cDNA clones of Langat tick-borne flavivirus that differ from their parent in peripheral neurovirulence. Virology 269:225–237. https://doi.org/10.1006/viro.2000.0220.
83. Mlera L, Meade-White K, Saturday G, Scott D, Bloom ME. 2017. Modeling Powassan virus infection in *Peromyscus leucopus*, a natural host. PLoS Negl Trop Dis 11:e0005346. https://doi.org/10.1371/journal.pntd.0005346.
84. Tsetsarkin KA, Liu G, Kenney H, Bustos-Arriaga J, Hanson CT, Whitehead SS, Pletnev AG. 2015. Dual miRNA targeting restricts host range and attenuates neurovirulence of flaviviruses. PLoS Pathog 11:e1004852. https://doi.org/10.1371/journal.ppat.1004852.
85. Barry G, Alberdi P, Schnettler E, Weisheit S, Kohl A, Fazakerley JK, Bell-Sakyi L. 2013. Gene silencing in tick cell lines using small interfering or long double-stranded RNA. Exp Appl Acarol 59:319–338. https://doi.org/10.1007/s10493-012-9598-x.